Fuel 243 (2019) 541–553

Contents lists available at ScienceDirect

Fuel

journal homepage: www.elsevier.com/locate/fuel

Full Length Article

A shock tube study of n-heptane, *iso*-octane, n-dodecane and *iso*-octane/n-dodecane blends oxidation at elevated pressures and intermediate temperatures

Jiankun Shao, Rishav Choudhary, Yuzhe Peng, David F. Davidson*, Ronald K. Hanson

Mechanical Engineering Department, Stanford University, Stanford, CA 94305, United States

ARTICLE INFO

Keywords:
Ignition delay
Shock tube
n-Heptane
Iso-octane
n-Dodecane
First-stage ignition

ABSTRACT

Ignition delay times (IDT) of n-heptane, *iso*-octane, n-dodecane, and *iso*-octane/n-dodecane blends, in stoichiometric mixtures with air, were measured behind reflected shock waves in a heated, high-pressure shock tube. Measurements were taken at temperatures of 665–1250 K, pressures of 28–70 atm, and equivalence ratios near unity. Pressure time-history recorded from sidewall piezo-electric transducers, fuel-concentration time-history obtained from fixed-wavelength laser absorption at 3.39 μm, and OH* (306 nm) emission time-history recorded by a Si detector, were used to determine IDT. The staged ignition phenomenon in the low temperature regime was also examined with attention on the 1st stage fuel decomposition fraction. IDT measurements were also made using the constrained-reactive-volume strategy, which has the capability to eliminate non-ideal effects such as remote ignition, and were compared with measurements using a conventional filling technique. The current measurements provide a wide range (28–70 atm) of ignition delay times for key surrogate fuels under practical engine conditions, and hence provide validation targets for refinement of chemical kinetic models.

1. Introduction

In support of the development of high-fidelity chemical kinetics models for distillate hydrocarbon fuels, a surrogate approach has often been employed that uses selected archetypal hydrocarbons to represent real fuel components. For example, *iso*-octane and n-heptane have been used as surrogates for gasoline [1–3] and n-dodecane has been used as a surrogate for jet fuel [4–6]. Because of this, there is a critical need for experimental kinetics databases that can be used for the validation and refinement of the mechanisms for these surrogates, especially at intermediate temperatures and elevated pressures of interest to engine modelers. Shock tube studies can contribute to these databases by providing both ignition delay time and species time-history measurements [7]. The current study aims to improve the knowledge of *iso*-octane, n-heptane, and n-dodecane oxidation chemistry by providing a reliable high-pressure, intermediate-temperature IDT database and by tracking their fuel decomposition during 1st stage ignition.

Ignition delay time measurements (IDT) of *iso*-octane/air mixtures have been extensively reported in the literature [8–12]. However, earlier research focused on relatively lower pressures and higher temperatures rather than the high pressures and intermediate temperatures found to exist in modern engines. Understanding of the staged-ignition phenomenon of *iso*-octane oxidation has also been lacking because the pressure rise during 1st stage ignition of *iso*-octane/air stoichiometric mixture is difficult to quantify and interpret at an equivalence ratio close to one [11]. *Iso*-octane chemistry has been investigated by detailed modeling [13,14], but there are still discrepancies in elevated-pressure IDT predictions. In the current work, we investigated *iso*-octane/air mixtures over a broad range of operating conditions. With careful sensitivity examinations of possible non-ideal effects, the current data provided a valuable database to validate the mechanisms at these conditions.

There has been a long history of n-heptane auto-ignition investigations in shock tubes. In one key early study, Ciezki et al. [15] conducted auto-ignition investigations for n-heptane/air mixtures under engine-relevant conditions. The initial pressure was varied between 3.2 and 42 bars and the initial temperature between 660 and 1350 K, while the equivalence ratio covered the region between 0.5 and 3.0. In another important study, Herzler et al. [16] measured ignition delay times of lean (Φ = 0.1–0.4) heptane/air mixtures in the temperature range 720 K < T < 1100 K at pressures of about 50 bar to determine auto-ignition characteristics under conditions relevant to diesel and homogeneous charge compression ignition (HCCI) engines, where two-stage ignition occurs. Loparo et al. [17] extended the n-heptane oxidation study to fuel

* Corresponding author at: Department of Mechanical Engineering, Stanford University, 418 Panama Mall, Room 104, Stanford, CA 94305-3032, United States.
E-mail address: dfd@stanford.edu (D.F. Davidson).

https://doi.org/10.1016/j.fuel.2019.01.152
Received 20 November 2018; Received in revised form 15 January 2019; Accepted 27 January 2019

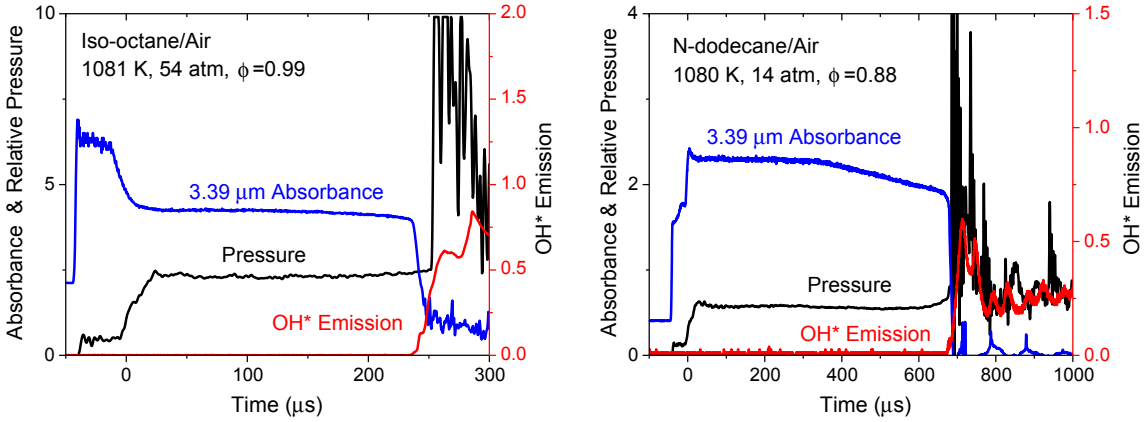

Fig. 1. Example ignition delay time measurements in the high-temperature range. Left frame: *iso*-octane/air ϕ = 0.99, 1081 K, 54 atm. Right frame: n-heptane/air ϕ = 0.88, 1080 K, 14 atm.

rich conditions. The study was conducted for n-heptane/O_2/Ar mixtures at equivalence ratios, ϕ, of 2.0 and 3.0, temperatures ranging from 1066 to 1502 K and pressures ranging from 1.4 to 6.2 atm. A series of studies of n-heptane auto-ignition has also been conducted at Stanford [18–22]. In the current study, the staged-ignition phenomenon of n-heptane along with IDT measurements of n-heptane/air mixtures at elevated pressures are investigated.

Only a limited number of n-dodecane oxidation studies have been reported in the literature [23,24], especially for gas-phase shock tube ignition delay times at elevated pressures. Vasu et al. [4] measured ignition delay times and OH concentration time histories during *n*-dodecane oxidation behind reflected shock waves using a heated, high-pressure shock tube. Measurements were conducted at temperatures of 727–1422 K, pressures of 15–34 atm, and equivalence ratios of 0.5 and 1.0. Another study at elevated pressures was conducted by Davidson et al. [25], which was aimed at measuring species time histories during n-dodecane oxidation. The concentration time-histories behind reflected shock waves were measured for five species: n-dodecane, C_2H_4, OH, CO_2, and H_2O. Other n-dodecane IDT studies were obtained from experiments performed on an aerosol shock tube (AST) [26,27]. In this study, we have investigated the IDT of n-dodecane at high pressures as well as that of n-dodecane/*iso*-octane mixtures, as little data are available on the synergistic effects of this binary fuel mixture.

2. Experimental methods

2.1. High-Pressure shock tube

Ignition delay time experiments for all test mixtures were performed using the Stanford high-purity, high-pressure shock tube (HPST). Typical uniform test times were of the order of 2 ms when helium was used as the driver gas. The stainless steel driven section had an internal diameter of 5 cm and was heated to 90C to prevent condensation of the test gas mixtures. Diaphragms were made of aluminum of 0.5–3.0 mm thickness (with cross-scribing) to allow measurements over a broad range of pressure (10–100 atm). The dP_5^*/dt (where $dP_5^* = dP_5/P_5$) values for current studies were negligible owing to use of a driver section insert that corrected for small changes in the non-reactive reflected shock pressure profiles.

The high-purity (~99%) n-heptane, *iso*-octane, and n-dodecane were obtained from Sigma-Aldrich. High-purity synthetic air (79% N_2, 21% O_2) is supplied by Praxair as the bath gas. To prepare the test gas mixture, the liquid fuel (neat or mixture) was injected into a heated 12.8-liter stainless-steel mixing tank at 110C. The test gas mixture of fuel/oxidizer was then prepared manometrically and was stirred using a magnetically driven vane assembly for at least 15 min before the experiments.

2.2. Shock tube diagnostics

Three diagnostics were employed during the experiments: laser absorption at 3.39 μm, excited OH radical (OH*) emission near 306 nm, and sidewall pressure. This experimental setup provided the capability of measuring both the *in situ* initial fuel loading (sometimes found to be slightly smaller than the manometric measurement in the mixing tank due to condensation losses in the transfer lines and shock tube walls), and the fuel decomposition time-history, as well as the bulk auto-ignition time. In all figures, laser absorption measurements are converted to absorbance using Beer's law for monochromatic radiation: $I/I_0 = \exp(-\sigma N L)$, where I/I_0 is the measured laser transmission through the shock tube, and the absorbance (σ N L) is linearly related to σ, the known fuel absorption cross-section, N, the number density of the absorbing fuel, and L, the shock tube diameter. Though some small amount of absorption from transient fuel decomposition products is expected, in this study we have assumed that the 3.39 μm absorption is dominated by the initial fuel.

The emission near 306 nm from OH* was detected using a modified Thorlabs™ PDA36A Si detector and Schott UG5 filter. Pressure time-histories in the test section were monitored using a Kistler™ piezoelectric pressure transducer model 603B1. The measurement location of all diagnostics was 1.1 cm away from the end wall.

Representative data traces for example ignition experiments in the high-temperature range are shown in Fig. 1; data include pressure traces for the reactive (fuel/oxidizer) cases together with the OH* emission records and 3.39 μm HeNe laser absorbance measurements. In this study, ignition delay time was defined as the time interval between the arrival of the reflected shock and the onset of ignition at the sidewall observation port determined by extrapolating the maximum slope of signals back to the baseline. Note that the measured sidewall IDT values can be slightly shorter (up to 20 μs) than end wall IDT values for ignition events with large energy release and immediate blast wave formation. In all cases, this approach provided consistent IDT among the three records. For consistency, the IDT data discussed in the following sections used the 3.39 μm laser absorption signal definition unless stated otherwise. The 2σ uncertainty of the high-temperature ignition delay data was typically ± 10%. This uncertainty was estimated by the theory of propagation of uncertainty with the primary contribution from the 2σ uncertainty of ± 1% in the initial reflected-shock temperature.

Since the NTC region behavior is a critical property of a fuel that can be related to engine knock [28], extra emphasis was laid upon acquiring repeatable data in the NTC temperature regime between 700 K and 950 K. Representative data traces for n-dodecane/air mixtures in the intermediate-temperature range with staged ignition are shown in Fig. 2. In this study, the 1st stage IDT was defined as the time interval

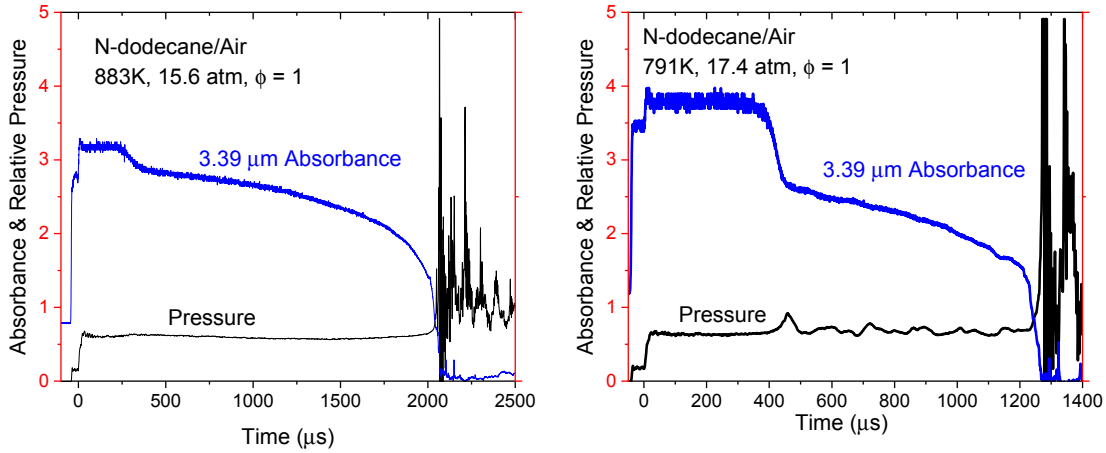

Fig. 2. Example ignition delay time measurements at intermediate temperature range. Left frame: n-dodecane/air ϕ = 1, 791 K, 17.4 atm. Right frame: n-dodecane/air ϕ = 1, 883 K, 15.6 atm.

between the arrival of the reflected shock and the 1st turning point of 3.39 μm laser absorbance signal, which was determined by extrapolating the maximum initial decrease slope of 3.39 μm signal back to the initial 3.39 μm signal baseline. In the intermediate temperature range (700–950 K), staged ignition was evident for n-alkanes as shown by the 3.39 μm signals in Fig. 2. In most of the cases, there was negligible pressure rise after 1st stage ignition, as shown in Fig. 2a. However, there were also cases with apparent pressure oscillations after 1st stage ignition, as shown in Fig. 2b and discussed in a later section. The overall IDT 2σ uncertainty in the intermediate temperature range was approximately 15%, with about 5% uncertainty coming from the pressure oscillations after 1st stage ignition.

3. Results and discussion

In Section 3.1, the IDT measurements for *iso*-octane/air mixtures are reported, and the constrained reaction volume (CRV) filling strategy data are compared with traditional shock tube filling strategy data. In Section 3.2, the IDT measurements for n-heptane/air mixture are reported and the stage-ignition phenomenon is examined using the 3.39 μm laser signal. In Section 3.3, the IDT measurements for n-dodecane/air mixtures are reported, and a similar oxidation process seen in n-heptane and n-dodecane is discussed. In Section 3.4, the IDT measurements for 50% *iso*-octane/50% n-dodecane/air mixtures are reported. In Section 3.5, the extent of non-ideal effects on the NTC region experiments is discussed.

3.1. Iso-octane ignition delay times

The IDT data for *iso*-octane/air mixtures are presented in Tables S1 and S2. The IDT measurements for *iso*-octane/air mixtures were conducted at temperatures of 665–1185 K, pressures of 25–70 atm and an equivalence ratio of 1 using a conventional filling method. To avoid remote ignition, additional experiments were performed using the CRV filling method [29,30] and used for comparison.

The IDT data of *iso*-octane/air using traditional filling are shown in Fig. 3. CHEMKIN-PRO simulations using a constant-volume constraint and the Lawrence Livermore National Laboratory (LLNL) gasoline surrogate mechanism [31] were compared with the measured data. The simulation results were consistent with the current measurements in the high-temperature range, however discrepancies appear at low temperatures for the 50 atm dataset. A recently published mechanism with improved thermochemistry and chemical kinetics, Atef et al. (2017) [32], is also shown in Fig. 3, showing improved agreement with the data.

At 50 atm, staged ignition was captured by the 3.39 μm signal in the

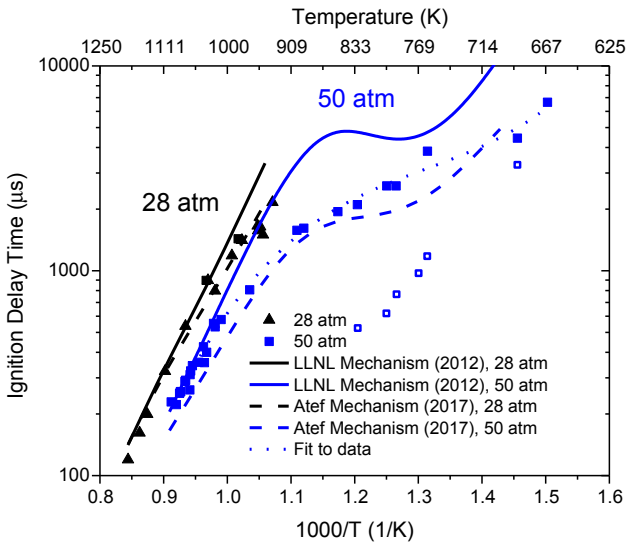

Fig. 3. *Iso*-octane/air IDT measurements: 28 and 50 atm, ϕ = 1.0. Blue squares: 50 atm, 2nd stage IDT; blue open squares: 50 atm, 1st stage IDT. Black triangles: 28 atm 2nd stage IDT. Solid lines: LLNL model, dashed lines: Atef et al. model, Dotted line: fit to 50 atm 2nd stage IDT data. (For interpretation of the references to colour in this figure legend, the reader is referred to the web version of this article.)

intermediate temperature region, which provided the 1st stage IDT data. The pressure rise after 1st stage ignition was negligible under current test conditions, and this observation was consistent with earlier studies [11,12].

To avoid non-ideal effects, such as remote ignition, the CRV filling strategy was applied to attain data at similar operating conditions. [29] The CRV strategy for conducting kinetics experiments behind reflected shock waves was achieved in the present work by staged filling. In a typical shock wave IDT experiment, the entire driven section of the shock tube is filled with test gases. However, in a CRV experiment using the staged filling method, only a small portion of the driven section is filled with test gases. In the current experiment, the CRV strategy was achieved by 15:1 stage filling, i.e. adding 15 volumes of inert gas after the initial filling volume of test gas mixture. In the first filling stage, the test mixture was filled into the shock tube to an initial pressure lower than the desired ultimate driven-section pressure. Then, in the second stage, a non-reactive gas (in this study, air) was filled into the driven section from a port near the diaphragm, compressing the reactive gas from the initial-stage fill to create a small slug of test gas near the end

wall. To minimize mixing between the non-reactive and reactive mixtures, the second-stage filling was done slowly such that the filling took place over 2–5 min. The most important variable in designing a stage filling experiment was the length of the reactive slug at the test section behind the reflected shock (L5), which was calculated by density ratio. For example, for an experiment at 1000 K and 28 atm, the density ratio of region 5 and region 1 is about 10, and 15:1 stage filling should yield a 3.3 cm long slug. The major concern using stage filling was the possible mixing of reactive gas and non-reactive gas in the test region, which was checked *in situ* and in real time with laser absorption at 3.39 μm.

There were several benefits by using the stage filling strategy. From hydrogen–oxygen ignition experiments, we noticed that this strategy eliminates the possibility of non-localized (remote) ignition in shock tubes. Furthermore, in mixtures with low energy release rates, the strategy can also effectively eliminate or minimize pressure changes due to combustion heat release, thereby enabling quantitative modeling of the kinetics throughout the combustion event using a simple assumption of specified pressure and enthalpy [29]. In the current study, high energy release rates occur and pressure changes significantly during ignition. Thus this case, constant-volume simulations are used to compare with measured data.

In Fig. 4, the IDT measurements using the traditional filling strategy are compared with the CRV-strategy data. The two datasets were consistent in the operating conditions. The simulations using a constant-volume model and two detailed mechanisms were also shown on the plot. The LLNL mechanism overpredicted the ignition delay times of *iso*-octane/air mixtures below 1000 K. The Atef et al. mechanism better predicts the measurement at lower temperatures.

In Fig. 5, results of the current study are compared with selected earlier literature studies. In the high temperature range, the current study is in good agreement with the literature studies from Shen et al. [8], Fieweger et al. [11,12] and Davidson et al. [9,10] at different pressures. The current work extended the test conditions to a lower temperature.

3.2. n-Heptane ignition delay times

The ignition delay times for n-heptane/air mixtures are presented in Tables S3 and S4. The IDT measurements for n-heptane/air mixtures were conducted at temperatures of 751–1127 K, pressures of 23–30 atm and an equivalence ratio of 1. The CRV strategy discussed in the last section was also used with a subset of the n-heptane data. Table S4 shows the CRV data.

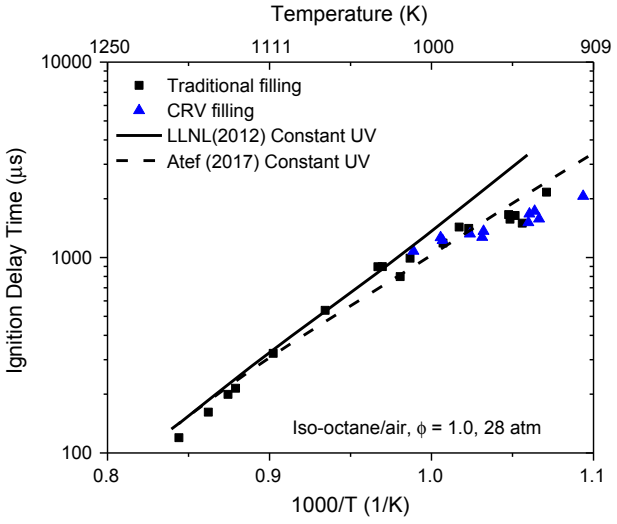

Fig. 4. Comparison between traditional filling and CRV filling. Solid lines: Simulations using the LLNL mechanism, Dash lines: Simulations using the Atef et al. mechanism.

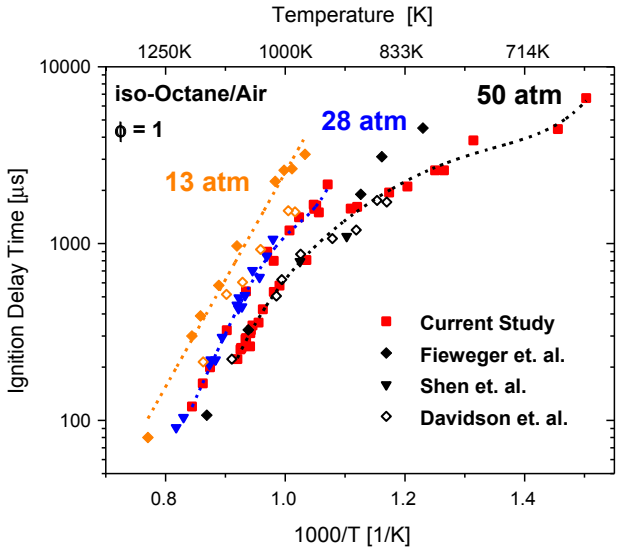

Fig. 5. Comparison between current study and literature studies for *iso*-octane/air mixtures. Orange points are the literature data near 13 atm, blue points are the literature data near 28 atm, and black points are the literature data near 50 atm. And, red points are current studies. Dashed lines: best fit. (For interpretation of the references to colour in this figure legend, the reader is referred to the web version of this article.)

n-Heptane ignition has been studied in the literature extensively; a comparison with selected studies is shown in Fig. 6. The current study is consistent with earlier studies at different pressures and in particular, is in good agreement with the 28 atm study from Ciezki et al. [14]. Combined with the literature data at different pressures, we found the pressure exponents in a IDT correlation (from 13 to 50 atm), $n = \ln(\tau_2/\tau_1)/\ln(P_2/P_1)$, is approximately −1.5 between 800 and 950 K and approximately −1.0 between 950 and 1100 K. As was evident in earlier studies there is an IDT peak shift with pressure in the NTC region [33].

Fig. 7 shows the current measurements and constant-volume simulations of n-heptane/air mixtures. The simulations were conducted using the LLNL gasoline surrogate mechanism and Zhang n-heptane detailed mechanism [34] using CHEMKIN. Excellent agreement between the traditional filling strategy and the CRV strategy data is seen in the 1st stage ignition delay times. In the NTC regime however, the

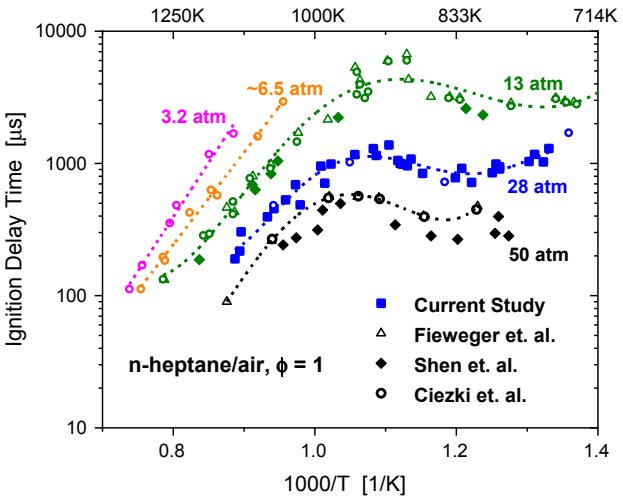

Fig. 6. Comparison between current results and literature data for n-heptane/air mixtures. Dashed lines: best fit to data.

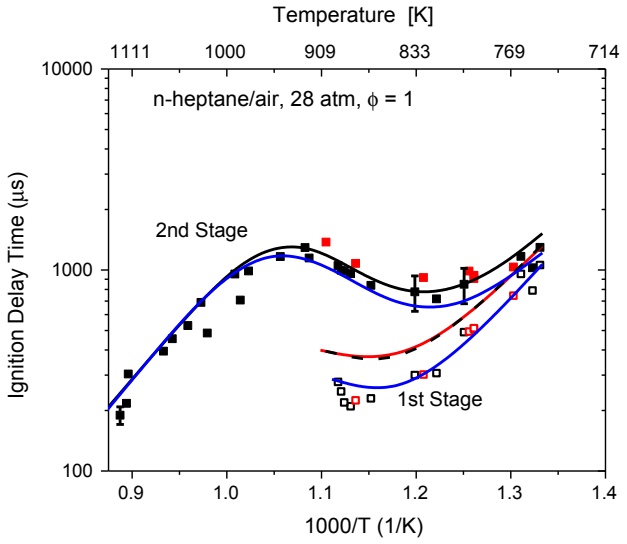

Fig. 7. Ignition delay time of n-heptane/air mixture. Modeling: black line, constant V model and LLNL (2012) mechanism; blue line, constant V model and Zhang (2016) mechanism. Data: red points, CRV data; black points, conventional filling data. (For interpretation of the references to colour in this figure legend, the reader is referred to the web version of this article.)

CRV strategy data has noticeably longer 2nd stage ignition delay times than traditional filling strategy data, primarily because of the reduced or suppressed pressure rises seen in the CRV data after the 1st stage ignition. Further examples of CRV and traditional filling are given in Fig. 10.

On Fig. 7, three different temperature zones can be identified on the basis of their 1st stage ignition behavior: the high temperature range (above 950 K) where no 1st stage ignition was captured by HeNe signal; the intermediate temperature range (950 K > T > 700 K) where an obvious 1st stage ignition was captured by the HeNe (3.39 μm) signal; and the low temperature range (below 700 K) where again no 1st stage ignition is expected. Both the mechanisms can predict the 2nd stage ignition delay time very well, and Zhang mechanism can better predict the 1st stage ignition delay time.

The fuel fraction remaining after the 1st stage ignition $F_{fuel}(t)$, is an important property of the fuel, especially in the engine operating conditions close to NTC region. Using a simplified interpretation of the absorbance signals, $F_{fuel}(t)$ can be related to the measured change in absorbance by the follow relation:

$$F_{fuel}(t) = N_{fuel}(t)/N_{fuel}(0) = (\alpha_{1st}/\alpha_0 - C)/(1-C)$$

where α_0 was the baseline absorbance at 3.39 μm by the test gas mixture, α_{1st} was the 1st stage ignition termination point absorbance, C is the ratio of the product and fuel cross-sections. The derivation of this relationship is given in the Appendix.

The 1st stage ignition termination point is defined as the extrapolation of max slope of the 3.39 μm signal during 1st stage ignition to the signal baseline after 1st stage ignition, as shown on Fig. 8. The fuel fraction remaining $F_{fuel}(t)$, is plotted against temperature in Fig. 9 and increases monotonically with temperature. At lower temperatures, the uncertainty of the measured fuel fraction remaining increases, as separation of the 1st and 2nd stage ignition decreases making the determination of the 1st stage ignition termination point more uncertain. When the initial temperature was lower than 750 K, no staged ignition was observed. The LLNL model, the red line in Fig. 9, and Zhang model, the blue line in Fig. 9, are both in good agreement with this simplified interpretation of the 3.39 μm laser absorption data.

To investigate the possible influence of remote ignition effects, n-heptane/air IDT experiments were also performed with using the CRV strategy. The 1st stage ignition delay time of CRV data are very consistent with traditional-strategy data. Slight differences in the 2nd stage ignition times are seen between the conventional-filling strategy data and CRV-filling strategy data that are likely the result of slightly different fuel loadings.

In Fig. 10, the pressure, OH* emission, and HeNe laser signals of the traditional measurements were compared to the CRV measurements. Consistent IDTs were observed for both cases. Both experiments were highly repeatable, which was achieved by careful cleaning and regular maintenance of the experimental facility. No random, non-ideal effects were observed. (This is discussed further in Section 3.5). Similar raw data are seen in ref. 4, in particular, the pressure trace was usually flat before 2nd stage ignition. Under these conditions, the constant-volume assumption is effectively valid as the 1st stage heat release was weak and did not modify the test environment. At lower temperatures, heat release during the 1st stage ignition causes pressure oscillations after 1st stage ignition, as shown in Fig. 10b. The pressure oscillations were more obvious at a lower initial temperature, because more fuel decomposed and more energy was released during the 1st stage ignition.

These pressure oscillations were highly repeatable, but they were not captured by zero-dimensional constant-volume simulations. From the numerous past investigations of the behavior of large hydrocarbons in the Stanford shock tube group, this phenomenon was observed only for large n-alkanes, such as n-heptane and n-dodecane. It was not observed for branched hydrocarbons, such as *iso*-octane. Regardless of interpretation, the effect of the pressure oscillation on the 2nd stage ignition needs to be quantified.

3.3. n-Dodecane ignition delay times

The ignition delay times for n-dodecane/air mixture are presented in Table S5. The IDT measurements for n-dodecane/air mixture were conducted at temperatures of 715–1288 K, pressures of 14–70 atm and equivalence ratio of 1. Ignition delay time measurement and simulations for n-dodecane/air mixtures are shown in Fig. 11 and 12. Constant-volume-constrained simulations were conducted using the detailed n-alkane mechanism from LLNL [35]. After 1st stage ignition, there is observable pressure rise, which shows the environment is close to a constant-volume environment. Differences between the measured data and simulation results are evident, especially in NTC region.

The current IDT measurement of n-dodecane/air mixture can be compared with a previous investigation in the same facility at a different pressure [4]. Vasu et al. (2009) conducted the first gas-phase n-dodecane/air mixture IDT measurement in the high pressure shock tube at Stanford, at an average pressure of 25 atm. The current study extended the literature studies to a wider pressure range: 17 and 60 atm.

Combined with the literature data at different pressures, we found the pressure exponents for IDT correlation, $n = \ln(\tau_2/\tau_1)/\ln(P_2/P_1)$, is about −1.5 when the temperature is above 950 K and at pressures from 17 atm to 60 atm. At lower temperatures (< 950 K), we found a similar pressure exponent when combining the current 15 atm data with the 28 atm data from Vasu et al. [4]. However, there is an IDT peak shift with pressure in the NTC region and a more sophisticated pressure scaling method is advised.

Pressure oscillations after 1st stage ignition were also observed in n-dodecane/air experiments. Fig. 13 shows a comparison of the pressure trace, from two different measurements taken at almost the same operating conditions. The close match between the two pressure traces and absorbance traces illustrated the good repeatability of the experiments. It worth noting that similar oscillations were obtained with n-heptane but not with *iso*-octane. This emphasizes the similarity of n-alkanes during oxidation. The pressure oscillations were stronger at a lower initial temperature, which, as discussed in an earlier section, was related to the greater fuel consumption in the 1st stage ignition. Further investigations are needed to understand these oscillations and how they should be modeled.

Using a similar analysis as was used with n-heptane, the fuel

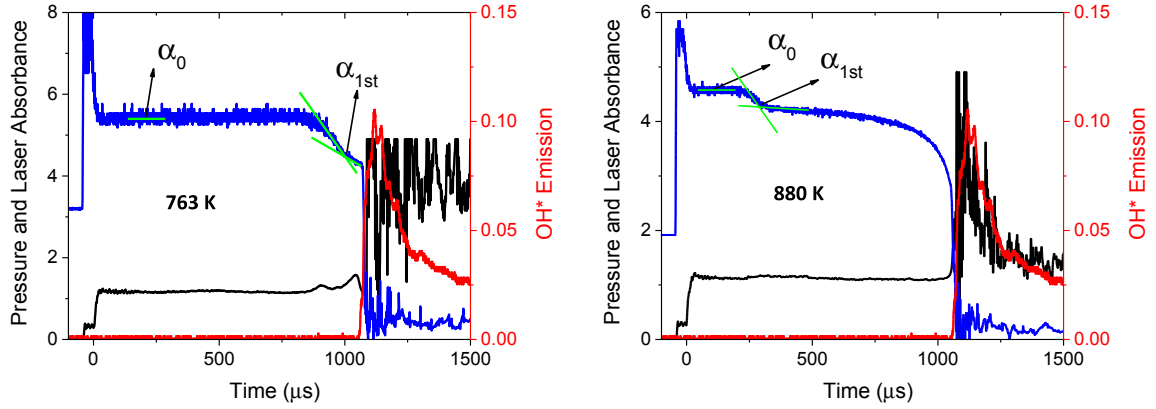

Fig. 8. Example n-heptane/air ignition experiments at 28 atm showing the baseline fuel absorbance α_0 and the 1st stage termination absorbance α_{1st} for 763 and 880 K.

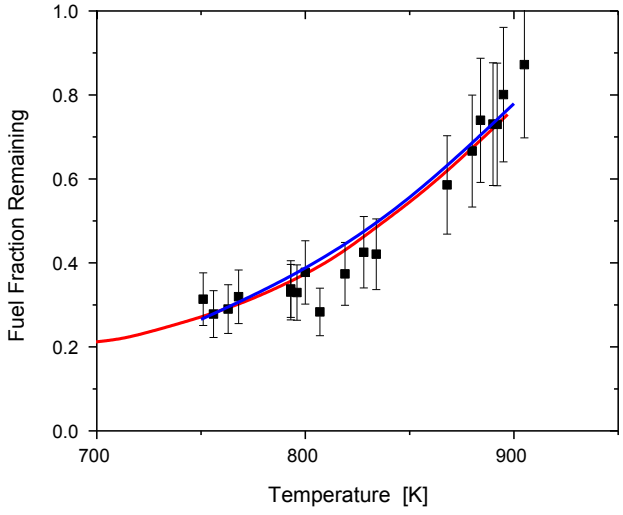

Fig. 9. Fuel fraction remaining after 1st stage ignition during n-heptane/air oxidation at 28 atm. Red line: LLNL (2016) constant V modeling; Blue line: Zhang (2016) constant V modeling. (For interpretation of the references to colour in this figure legend, the reader is referred to the web version of this article.)

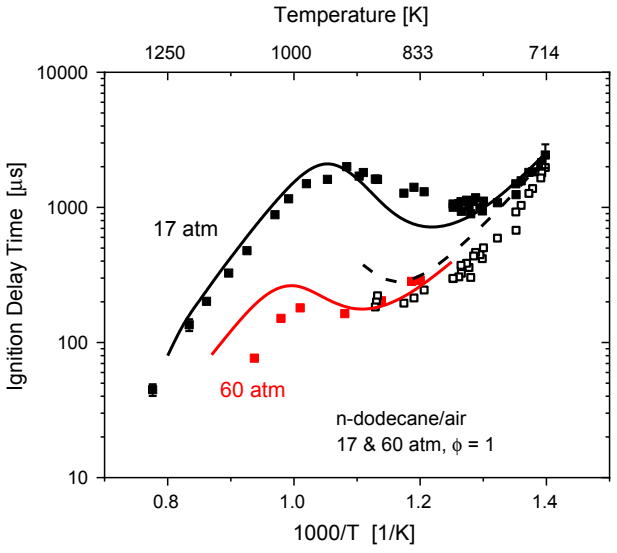

Fig. 11. n-Dodecane/air ignition delay time measurements and simulations. Solid symbols: 2nd stage IDT, open symbols; 1st stage IDT. Solid and dashed lines: LLNL constant V modeling. [35]

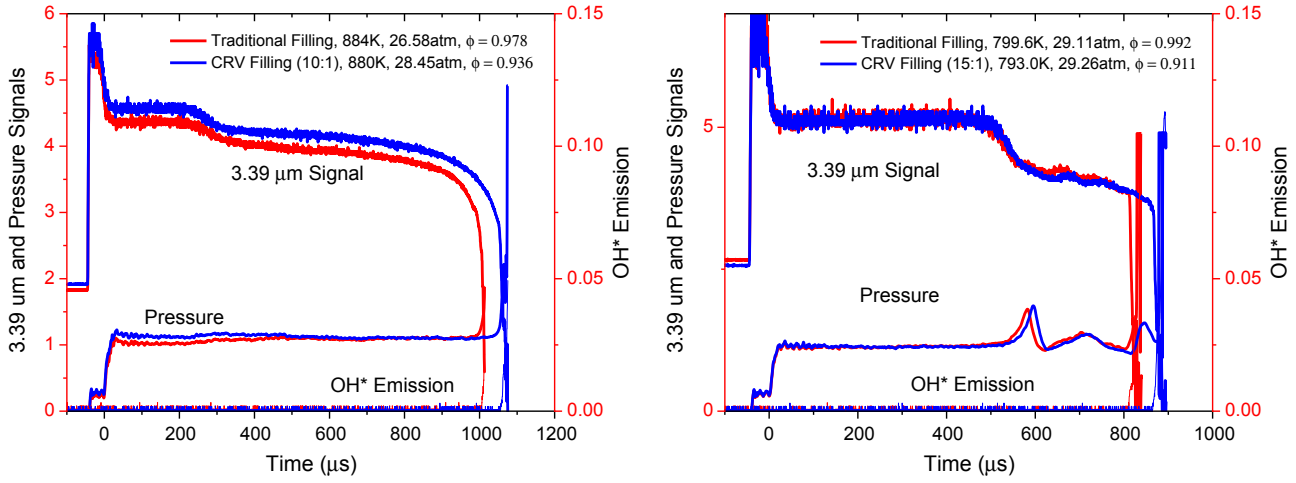

Fig. 10. Comparison of the pressure, OH* emission, and 3.39 absorbance data for reflected shock wave n-heptane/air experiments at similar test conditions but with different shock tube filling strategies: conventional-filling or CRV filling strategies. Left frame: 880 K and 27 atm; Right frame: 795 K, and 29.2 atm.

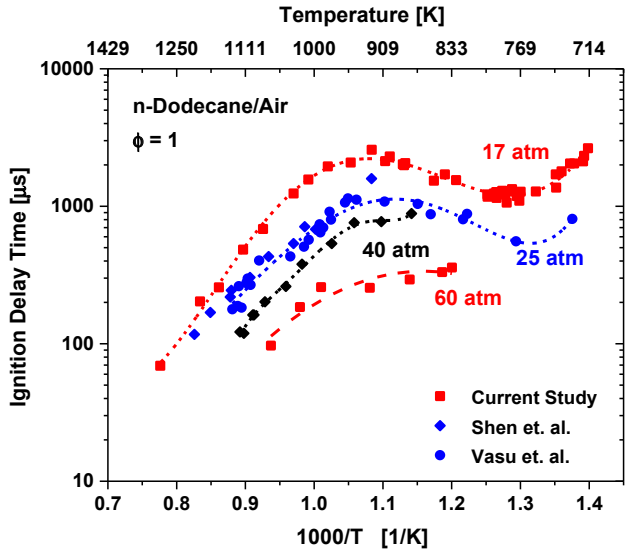

Fig. 12. Comparison between current data and earlier investigations for n-dodecane/air mixtures. Dashed lines are fit to data.

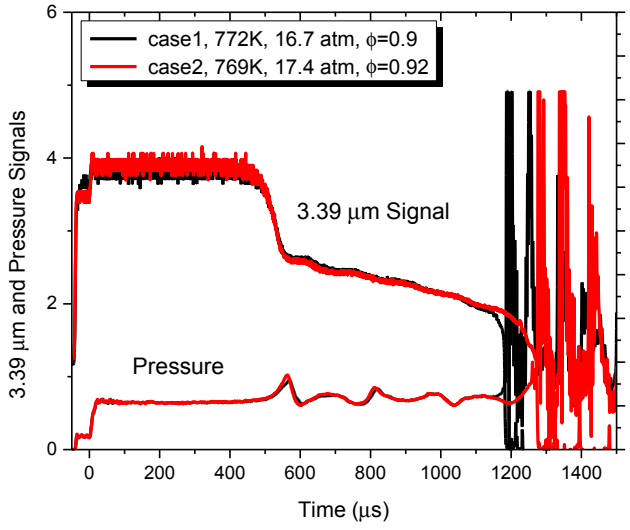

Fig. 13. HeNe laser and pressure signals during n-dodecane/air oxidation.

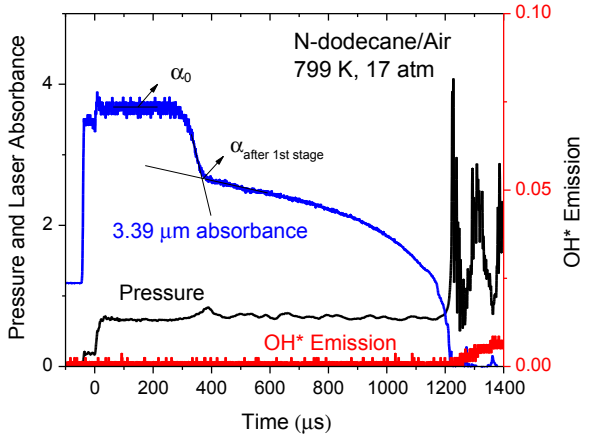

Fig. 14. Example n-dodecane/air ignition experiments at 17 atm showing the baseline fuel absorbance α_0 and the 1st stage termination absorbance α_{1st} for 799 K.

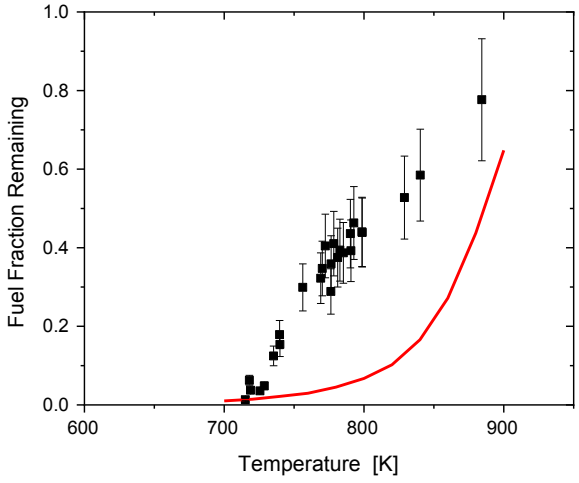

Fig. 15. Fuel fraction remaining after 1st stage ignition for n-dodecane/air mixture at 17 atm. Line: LLNL constant V modeling.

fractions remaining after 1st stage ignition in n-dodecane/air mixtures are shown in Figs. 14 and 15. The definition of the fuel fraction remaining is given in the n-heptane section and the detailed derivation of this relationship is given in the Appendix. The LLNL model simulations were in good agreement with this simplified interpretation of the 3.39 μm laser absorption data for n-heptane. The fuel fraction remaining of n-dodecane, however, has an approximately linear relation with temperature from 700 K to 900 K, which was not captured by simulations. In Fig. 15, the red line shows the LLNL constant-volume modeling, and it clearly underpredicts the measured fuel fraction remaining.

3.4. *Iso*-octane/n-dodecane blend ignition delay times

The ignition delay times for *iso*-octane/n-dodecane/air mixtures are presented in Table S6. The fuel mixture used was an equimolar mixture of n-dodecane and *iso*-octane. The ignition delay time measurements for the mixture were conducted in the temperature range of 748 to 1149 K, at pressures near 17 atm, and an equivalence ratio of 1.

Fig. 16 shows the IDT measurements of n-dodecane/*iso*-octane

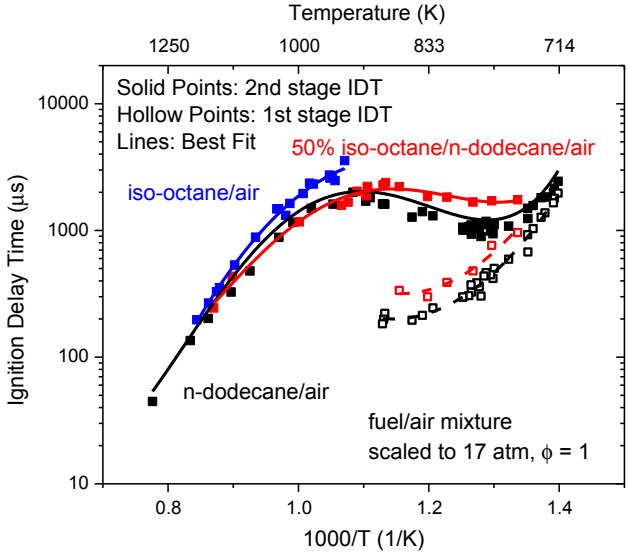

Fig. 16. Ignition delay times in air at 17 atm, ϕ = 1, for *iso*-octane, n-dodecane, and *iso*-octane/n-dodecane mixtures.

mixtures and compares those with the neat *iso*-octane/air and n-dodecane/air mixtures. The ignition delay times of *iso*-octane/air mixtures were larger than for n-dodecane/air mixtures at these test conditions, and the 50% *iso*-octane/ 50% n-dodecane/air mixture results were closer to the n-dodecane/air mixture than the *iso*-octane/air mixture, as the overall reaction rate of the mixture usually follows the fastest channel. In addition, the 50% *iso*-octane/ 50% n-dodecane/air mixture had a less obvious NTC behavior than for n-dodecane/air mixture, as expected.

Comparing the 1st stage ignition behavior of the two fuel mixtures, it is evident that the n-dodecane/air mixture had a shorter 1st stage ignition time than the blended mixture. The 1st stage ignition delay times for the blend appears to simply scale up and mimic the trend of the 1st stage IDT of the dodecane fuel. This shows *iso*-octane was more likely to work as a diluent during the 1st stage ignition, and was not opening new or closing existing chemical pathways prior to 1st stage ignition.

3.5. Non-ideal effects

In this study, the authors have tried to provide highly repeatable intermediate-temperature data with well-defined uncertainties. An important part of this study, therefore, is an examination of non-ideal effects, and their impact on the oxidation behavior of hydrocarbons.

Impurities has been known to have a significant effect on shock tube experiments [36]. In this study, all measurements were repeated after physical cleaning using acetone and after chemical cleaning using *tert*-butyl-hydro-peroxide (TBHP) [37]. The agreement of the measurements taken at similar operating conditions confirmed the repeatability of the results and also excluded impurity effects on current measurements.

Thermal boundary layer ignition was another non-ideal effect that can cause a significant uncertainty in NTC region IDT data [38]. The boundary layer temperature is usually lower than that existing in the core of the shock tube, and hence ignition may begin in the boundary layer for NTC region cases, where the ignition delay time is shorter at a relatively lower temperature. When this happens, the pressure transducer should reveal a smooth pressure rise before core auto-ignition due to flame propagation. Also, the OH* emission detector should record a similar smooth rise before core auto-ignition. The diagnostics used in this study were sufficiently sensitive to sense these effects. However, thermal boundary layer ignition was not observed.

Another possible effect is non-ideal hot-spot ignition, where some residual radicals or diaphragm pieces act as a source of flamelets, leading to a strong inhomogeneous ignition. This phenomenon was commonly observed when the test time was long (> 5 ms) [39]. When the shock tube test time was short (< 5 ms), the ignition was typically very uniform [39]. This was also the reason why was it desirable to do the NTC region ignition delay time measurements at high pressures. The IDTs are shorter at high pressures, and less likely to be affected by non-ideal effects. In addition, randomly distributed hot-spot induced ignition is expected to generate large scatter in the data. The high repeatability of the current data illustrated that non-ideal hot-spot ignition was not likely an issue in the current study.

4. Conclusion

Gas-phase ignition delay times of *iso*-octane/air mixture, n-heptane/air mixture, n-dodecane/air mixture and 50% *iso*-octane/50% n-dodecane/air mixture were measured in the Stanford high-pressure shock tube. The current measurements help the understanding of low temperature chemistry and will aid the development and validation of surrogate mechanisms. 1st stage fuel consumption was measured and found to agree with the model predictions for n-heptane oxidation at 28 atm. However, the model predictions for n-dodecane 1st stage fuel consumption using the LLNL n-dodecane mechanism overpredicted the measured results for most test conditions. Highly repeatable pressure oscillations after 1st stage ignition were observed for n-heptane and n-dodecane in the NTC region, which were not evident in the simulations. The observations and results summarized in this paper emphasize the need to further improve the low-temperature chemistry of these fuels.

Acknowledgements

This work was supported by the Air Force Office of Scientific Research through AFOSR Grant No. FA9550-14-1-0235, with Dr. Chiping Li as contract monitor.

Appendix A

Table S1
Ignition delay time of *iso*-octane/air mixture.

T5 (K)	P5 (atm)	phi	Ign_P (μs)	Ign_OH* (μs)	Ign_3.39	Ign_1st
iso-octane/air, P5 ~ 28 atm, phi = 1						
934	28	1.07	2166	2159	2142	
947	28.1	1.06	1512	1497	1503	
951	28.9	1.05	1595	1590	1584	
954	28	1.05	1594	1571	1586	
955	28.4	1.05	1635	1634	1625	
978	28	1.02	1426	1411	1412	
983	28.4	1.02	1424	1412	1416	
993	27.8	1.01	1197	1195	1188	
1013	26.8	0.99		1036	1035	
1020	27.3	0.98	826	818	814	
1031	27.1	0.97	945	930	934	
1034	28.2	0.97	908	892	891	
1070	26.4	0.93	573	569	563	
1108	26.5	0.9	351	342	347	
1138	25	0.88		240	239	
1144	25.6	0.87	230	218	224	
1160	25	0.86	201	181	193	
1185	25	0.84	144	134	144	

(*continued on next page*)

Table S1 (*continued*)

T5 (K)	P5 (atm)	phi	Ign_P (μs)	Ign_OH* (μs)	Ign_3.39	Ign_1st
iso-octane/air, P5 = 45–70 atm, phi = 1						
665	41.9	1.02	6644		6646	
687	45.2	0.91	4441		4442	3288
716	68.3	0.7	4686	4680	4684	3063
717	70	0.79	3692	3707	3707	2644
726	67.4	0.85	2989	2986	2993	1753
761	40.7	0.97	3834		3834	1178
770	43.4	1.1	2413		2413	973
790	50.1	1.02	2592		2595	768
800	47.8	1.04	2594		2595	619
830	53.1	1.01	2102		2102	525
852	51.5	1.01	1944		1943	
893	53.1	1.02	1613		1613	
901	51.6	1.01	1575		1576	
918	61.3	0.91	1966	1990	1984	
966	55.3	1	807	796	797	
1010	45.8	0.99	578	567	562	
1019	49.7	0.93	532.4	525	520	
1022	58.8	1	478	470	464	
1034	52	0.97	394	385	382	
1037	48.5	0.98	372	367	360	
1039	49.1	0.98	425	415	418	
1047	50.6	1.05	357	350	350	
1058	51.4	0.98	344	334	334	
1061	51.9	1	324	312	314	
1062	52	1	311	301	304	
1062	51.9	0.99	262	257	254	
1070	52.6	0.99	292	281	284	
1071	52	0.95	288	280	282	
1079	53.9	0.99	257	252	247	
1080	53.6	0.99	256	250	246	
1081	53.8	0.99	252	242	245	
1087	54.1	0.96	222	215	216	
1097	55.6	0.98	213	206	202	

Table S2
Ignition delay time of *iso*-octane/air mixture using CRV strategy.

T5 (K)	P5 (atm)	phi	Ign_OH* (μs)	Ign_3.39 μm (μs)
iso-octane/air, P5 ~ 28 atm, phi = 1, CRV Strategy				
914	27.7	0.91	2084	2102
938	27.1	0.87	1627	1609
940	27.3	0.88	1771	1769
943	27.9	0.91	1680	1669
944	27.4	0.85	1545	1666
969	26.7	0.91	1430	1416
970	27.4	0.98	1299	1266
977	27.5	0.93	1344	1319
993	27.0	0.91	1269	1334
994	27.0	0.90	1312	1221
1011	26.0	0.84	1163	1153

Table S3
Ignition delay times of n-heptane/air mixture.

T5 (K)	P5 (atm)	phi	Ign_P (μs)	Ign_OH* (μs)	Ign_3.39 μm (μs)	Ign_1st (μs)
n-heptane/air, P5 ~ 28 atm, phi = 1						
751	31.5	0.90	1165	1152	1158	941
756	30.5	0.92	958	941	945	726
763	30.3	1.01	1087	1082	1078	884
800	29.1	0.99	829	816.8	818	472
819	28.1	0.98	729	716.4	722	306
834	27.4	0.99	806	796.8	800	307
868	28.0	1.01	844	839.6	842	230
884	26.6	0.98	1014	1010	1012	221
890	27.2	1.01	1018	1016	1018	226
892	28.3	1.12	981	987	981	246
895	26.2	1.00	1144	1126	1140	297
920	26.8	1.02	1216	1199	1178	
924	26.8	0.98	1362	1349	1338	
947	25.5	1.00	1280	1281	1276	
978	25.8	0.98	1075	1072	1075	
986	28.3	1.00	690	701	690	
992	27.8	1.07	973	962	964	
1021	26.4	0.92	517	514.4	517	
1028	27.2	0.96	709	710.8	709	
1043	28.5	1.01	508.8	520	508.8	
1061	24.7	0.90	523	515.6	516	
1072	26.7	1.06	425	414	416	
1116	28.7	1.00	312	296	304	
1119	23.8	0.98	254	254.8	247	
1127	24.3	0.98	229	218	220	

Table S4
Ignition delay time of n-heptane/air mixture using CRV strategy.

T5 (K)	P5 (atm)	phi	Ign_P (μs)	Ign_OH* (μs)	Ign_3.39 μm (μs)	Ign_1st(μs)
n-heptane/air, P5 ~ 28 atm, phi = 1, CRV						
768	29.6	0.96	988	978.4	980	705
793	29.0	0.89	915	908.4	908	490
793	29.3	0.91	879	868	870	491
796	29.0	0.83	961	954.8	960	477
828	28.5	0.92	907	899.6	900	387
880	28.5	0.94	1074	1061	1069	296
905	28.0	0.92	1395	1378	1387	221

Table S5
Ignition delay time of n-dodecane/air mixture.

T5 (K)	P5 (atm)	phi	Ign_P (μs)	Ign_OH* (μs)	Ign_3.39 μm (μs)	Ign_1st (μs)
n-dodecane/air, P5 ~ 28 atm, phi = 1						
715	18.5	0.86	2641		2641	1814
718	18.4	0.93	2324		2304	1654
719	18.7	1.04	2120		2129	1504
726	17.9	0.80	2048		2037	1307
729	17.7	0.85	2047		2029	1218
735	17.5	0.84	1794	1791	1794	1003
740	18.2	0.97	1365	1357	1366	632
740	17.5	0.92	1706	1705	1708	897
756	16.9	0.96	1280	1280	1280	595.6
769	17.4	0.92	1275	1271	1275	489
770	17.2	0.88	1097	1089	1094	413
772	16.7	0.90	1186	1182	1183	455
776	17.7	0.90	1331	1328	1333	446
778	17.2	0.97	1287	1288	1285	431.2
781	16.9	0.93	1062	1056	1052	305.2
783	16.9	0.96	1218	1229	1213	360
785	17.4	0.95	1295	1288	1290	376
790	16.3	0.97	1150	1152	1141	340
791	17.4	0.97	1267	1271	1263	364
793	17.2	1.01	1238	1226	1233	302
799	17.1	0.95	1173	1170	1167	295
799	17.4	0.98	1220	1228	1213	292

(*continued on next page*)

Table S5 (*continued*)

T5 (K)	P5 (atm)	phi	Ign_P (μs)	Ign_OH* (μs)	Ign_3.39 μm (μs)	Ign_1st (μs)
829	16.8	0.86	1550	1595	1538	247
840	16.5	0.86	1704	1744	1698	220
852	16.6	0.97	1534	1532	1534	200
883	15.6	0.95	2061	2051	2062	241
884	16.3	0.95	1987	1970	1952	208
886	16.1	0.93	2018	2122	2018	194
901	15.7	0.95	2302	2257	2283	
906	16.0	0.96	2130	2109	2117	
923	15.5	0.94	2575	2540	2602	
949	15.5	0.93	2080	2031	2065	
981	15.4	0.94	1948	1935	1946	
1008	14.8	0.91	1566	1556	1562	
1031	14.2	0.93	1239	1230	1232	
1080	14.0	0.88	683	678	683	
1115	13.5	0.90	484	480	483	
1161	15.7	0.95	257	241	246	
1199	13.3	0.90	203	195	193	
1288	12.9	0.87	69.2	60	60.8	
n-dodecane/air, P5 = 50–70 atm, phi = 1						
833	68.4	0.70	358	370	406	
843	65.3	0.79	332	338	357	
878	51.0	0.75	293	329	306	
925	57.1	0.74	255	248	255	
990	58.6	0.78	258	243	260	
1021	57.3	0.92	185	175	184	
1067	52.9	1.02	97	87	97	

Table S6
Ignition delay time of 50% *iso*-octane/ 50% n-dodecane/air mixture.

T5 (K)	P5 (atm)	phi	Ign_P (μs)	Ign_OH* (μs)	Ign_3.39 μm (μs)
50% *iso*-octane/50% n-dodecane/air, P5 ~ 17 atm, phi = 1					
748	21.6	1.02	1373	1373	1373
771	21.6	1.01	1347	1333	1342
789	20.2	1.04	1412	1405	1406
815	20.2	1.02	1540	1547	1540
835	19.9	1.06	1585	1601	1582
866	17.7	1.06	2125	2109	2106
882	16.5	1.05	2464	2421	2437
885	13.7	1.03	2832	2825	2817
904	14.6	1.06	2501	2507	2473
904	15.3	1.04	2473	2452	2471
906	13.4	1.04	2379	2361	2353
918	14.6	1.03	2362	2336	2338
929	14.9	1.02	1904	1895	1901
938	12.7	1.02	2113	2095	2095
998	15.9	1.01	1250	1237	1242
1113	14.3	0.96	517	510	516
1149	12.4	0.98	334	322	331

Appendix B:. Relating $F_{fuel}(t)$ to 3.39 μm absorbance time history

In the paper, fuel fraction remaining after 1st stage ignition is given by:

$$F_{fuel}(t) = N_{fuel}(t)/N_{fuel}(0) = (\alpha_{1st}/\alpha_0 - C)/(1-C)$$

where α_0 was the baseline absorbance at 3.39 μm by the test gas mixture, α_{1st} was the 1st stage ignition termination point absorbance at 3.39 μm, C is the ratio of the product and fuel absorption cross-sections. The derivation of the equation is given below.

Because the fuel diagnostic relies on the mid-infrared HeNe laser (3.39 μm), which is absorbed by the C—H stretch band of the fuel, any species containing similar C—H bonds will also absorb at the HeNe laser wavelength and complicate the direct interpretation of the fuel measurement. Here we use a simple model to estimate the fuel number density from the 3.39 μm laser absorption data.

$$fuel \xrightarrow{k} products$$

where "fuel" and "products" are each described as a single absorbing component and k is the rate at which this reaction proceeds. At time t = 0, only fuel exists and at time t = τ_1, the mixture of fuel and products exist. Therefore, the rate of removal of the fuel concentration (N_f) and of product formation (N_p) are:

$$\frac{dN_f}{dt} = -kN_f; \frac{dN_p}{dt} = kN_f$$

At any given time, the measured absorbance is composed of a contribution from fuel plus a contribution from products:

$$\alpha_{meas}(t) = \alpha_f(t) + \alpha_p(t)$$

$$= \sigma_f N_f(t)L + \sigma_p N_p(t)L$$

$$= \sigma_f N_f(t)L + \sigma_p(N_f(0) - N_f(t))L$$

$$= \sigma_f N_f(t)L + C\sigma_f(N_f(0) - N_f(t))L$$

where C = (σ_p/σ_f) is the ratio of the absorption cross-sections for fuel and products at 3.39 μm, and we have assumed this ratio is constant at all relevant temperatures and times. Rearranging the terms and normalizing $\alpha_{meas}(t)$ with $\alpha_{meas}(0)$, we find that

$$\alpha_{meas}(t)/\alpha_{meas}(0) = N_f(t)/N_f(0) + C\,(1 - N_f(t)/N_f(0))$$

Rearranging we find that

$$F_{fuel}(t) = N_f(t)/N_f(0) = (\alpha_{meas}(t)/\alpha_{meas}(0) - C)/(1-C)$$

we are left to estimate a value for C. We note that at the lowest temperatures, the fuel consumption is completely dominated by 1st stage chemistry, and as the reaction temperature drops the 1st stage and final (i.e. 2nd stage) ignition become the same. Thus we assume as the lower temperatures, all of the fuel is converted to products during 1st stage ignition. This assumption is completely consistent with the LLNL simulations. In the case of n-dodecane, almost all the fuel has been consumed during the 1st stage ignition at 715 K. Thus, we can use the following equation to estimate C.

$$F_{fuel}(1^{st}) = N_f(1^{st})/N_f(0) = 0 = (\alpha_{meas}(1^{st})/\alpha_{meas}(0) - C)/(1-C)$$

Resulting in a value of C = 0.51.

For n-heptane, Fig. 10 shows the temperature where all fuel can be consumed during 1st stage ignition is out of the range of our current test. However, the simulation using LLNL gasoline mechanism shows the slope of 1st stage fuel consumption ratio change at low temperatures is small, initial temperature change from 600 K to 700 K only caused 7% 1st stage fuel consumption ratio change. Thus, we can estimate the C value for n-heptane at the lowest measured temperature case using the simulated fuel fraction remaining. For n-heptane, the value of C = 0.77.

References

[1] Gauthier BM, Davidson DF, Hanson RK. Shock tube determination of ignition delay times in full blend and surrogate fuel mixtures. Combust Flame 2004;139(4):300–11.

[2] Callahan CV, Held TJ, Dryer FL, Minetti R, Ribaucour M, Sochet LR, et al. Experimental data and kinetic modeling of primary reference fuel mixtures. Proc Combust Inst 1996;26(1):739–46.

[3] Shao J, Rutland CJ. Modeling investigation of different methods to suppress engine knock on a small spark-ignition engine. J Eng Gas Turbines Power 2015;137(6):061506.

[4] Vasu SS, Davidson DF, Hong Z, Vasudevan V, Hanson RK. n-Dodecane oxidation at high-pressures: Measurements of ignition delay times and OH concentration time-histories. Proc Combust Inst 2009;32(1):173–80.

[5] You X, Egolfopoulos FN, Wang H. Detailed and simplified kinetic models of n-dodecane oxidation: The role of fuel cracking in aliphatic hydrocarbon combustion. Proc Combust Inst 2009;32(1):403–10.

[6] Violi A, Yan S, Eddings EG, Sarofim AF, Granata S, Faravelli T, et al. Experimental formulation and kinetic model for JP-8 surrogate mixtures. Combust Sci Technol 2002;174(11–12):399–417.

[7] Shao J, Zhu Y, Wang S, Davidson DF, Hanson RK. A shock tube study of jet fuel pyrolysis and ignition at elevated pressures and temperatures. Fuel 2018;226:338–44.

[8] Shen HPS, Vanderover J, Oehlschlaeger MA. A shock tube study of iso-octane ignition at elevated pressures: The influence of diluent gases. Combust Flame 2008;155(4):739–55.

[9] Davidson DF, Gauthier BM, Hanson RK. Shock tube ignition measurements of iso-octane/air and toluene/air at high pressures. Proc Combust Inst 2005;30(1):1175–82.

[10] Davidson DF, Oehlschlaeger MA, Herbon JT, Hanson RK. Shock tube measurements of iso-octane ignition times and OH concentration-time histories. Proc Combust Inst 2002;29(1):1295–301.

[11] Fieweger K, Blumenthal R, Adomeit G. Shock-tube investigations on the self-ignition of hydrocarbon-air mixtures at high pressures. Proc Combust Inst 1994;25(1):1579–85.

[12] Fieweger K, Blumenthal R, Adomeit G. Self-ignition of SI engine model fuels: a shock tube investigation at high pressure. Combust Flame 1997;109(4):599–619.

[13] Curran HJ, Gaffuri P, Pitz WJ, Westbrook CK. A comprehensive modeling study of iso-octane oxidation. Combust Flame 2002;129(3):253–80.

[14] Jia M, Xie M. A chemical kinetics model of iso-octane oxidation for HCCI engines. Fuel 2006;85(17):2593–604.

[15] Ciezki HK, Adomeit G. Shock-tube investigation of self-ignition of n-heptane-air mixtures under engine related conditions. Combust Flame 1993;93(4):421–33.

[16] Herzler J, Jerig L, Roth P. Shock tube study of the ignition of lean n-heptane/air mixtures at intermediate temperatures and high pressures. Proc Combust Inst 2005;30(1):1147–53.

[17] Loparo ZE, Lopez JG, Neupane S, Partridge Jr WP, Vodopyanov K, Vasu SS. Fuel-rich n-heptane oxidation: A shock tube and laser absorption study. Combust Flame 2017;185:220–33.

[18] Davidson DF, Hong Z, Pilla GL, Farooq A, Cook RD, Hanson RK. Multi-species time-history measurements during n-heptane oxidation behind reflected shock waves. Combust Flame 2010;157(10):1899–905.

[19] Horning DC, Davidson DF, Hanson RK. Study of the high-temperature autoignition of n-alkane/O/Ar mixtures. J Propul Power 2002;18(2):363–71.

[20] Campbell MF, Wang S, Goldenstein CS, Spearrin RM, Tulgestke AM, Zaczek LT, et al. Constrained reaction volume shock tube study of n-heptane oxidation: Ignition delay times and time-histories of multiple species and temperature. Proc Combust Inst 2015;35(1):231–9.

[21] Hong Z, Davidson DF, Vasu SS, Hanson RK. The effect of oxygenates on soot formation in rich heptane mixtures: a shock tube study. Fuel 2009;88(10):1901–6.

[22] Campbell, M. F., Wang, S., Davidson, D. F., & Hanson, R. (2018). Shock tube study of normal heptane first-stage ignition near 3.5 atm. Submitted to Combustion and Flame August 2018.

[23] Kadota T, Hiroyasu H. Spontaneous ignition delay of a fuel droplet in high-pressure and high-temperature gaseous environments. Bullet JSME 1976;19(130):437–45.

[24] Segawa D, Kadota T, Kohama R, Enomoto H. Ignition of binary mixture droplets by a propagating laminar flame. Proc Combust Inst 2000;28(1):961–8.

[25] Davidson DF, Hong Z, Pilla GL, Farooq A, Cook RD, Hanson RK. Multi-species time-history measurements during n-dodecane oxidation behind reflected shock waves. Proc Combust Inst 2011;33:151–7.

[26] Davidson DF, Haylett DR, Hanson RK. Development of an aerosol shock tube for kinetic studies of low-vapor-pressure fuels. Combust Flame 2008;155(1):108–17.

[27] Haylett DR, Davidson DF, Hanson RK. Ignition delay times of low-vapor-pressure

fuels measured using an aerosol shock tube. Combust Flame 2012;159(2):552–61.
[28] Wang Z, Liu H, Reitz RD. Knocking combustion in spark-ignition engines. Prog Energy Combust Sci 2017;61:78–112.
[29] Hanson RK, Pang GA, Chakraborty S, Ren W, Wang S, Davidson DF. Constrained reaction volume approach for studying chemical kinetics behind reflected shock waves. Combust Flame 2013;160(9):1550–8.
[30] Hanson RK, Davidson DF. Recent advances in laser absorption and shock tube methods for studies of combustion chemistry. Prog Energy Combust Sci 2014;44:103–14.
[31] Mehl M, Pitz WJ, Westbrook CK, Curran HJ. Kinetic modeling of gasoline surrogate components and mixtures under engine conditions. Proc Combust Inst 2011;33(1):193–200.
[32] Atef N, Kukkadapu G, Mohamed SY, Al Rashidi M, Banyon C, Mehl M, et al. A comprehensive iso-octane combustion model with improved thermochemistry and chemical kinetics. Combust Flame 2017;178:111–34.
[33] Uygun Y. Ignition studies of undiluted diethyl ether in a high-pressure shock tube. Combust Flame 2018;194:396–409.
[34] Zhang K, Banyon C, Bugler J, Curran HJ, Rodriguez A, Herbinet O, et al. An updated experimental and kinetic modeling study of n-heptane oxidation. Combust Flame 2016;172:116–35.
[35] Sarathy SM, Westbrook CK, Mehl M, Pitz WJ, Togbe C, Dagaut P, et al. Comprehensive chemical kinetic modeling of the oxidation of 2-methylalkanes from C7 to C20. Combustion Flame 2011;158(12):2338–57.
[36] Urzay J, Kseib N, Davidson DF, Iaccarino G, Hanson RK. Uncertainty-quantification analysis of the effects of residual impurities on hydrogen–oxygen ignition in shock tubes. Combust Flame 2014;161(1):1–15.
[37] Pang GA. Experimental determination of rate constants for reactions of the hydroxyl radical with alkanes and alcohols (Doctoral dissertation). Stanford University; 2012.
[38] Jayachandran J, Egolfopoulos FN. Thermal and Ludwig-Soret diffusion effects on near-boundary ignition behavior of reacting mixtures. Proc Combust Inst 2017;36(1):1505–11.
[39] Tulgestke AM, Johnson SE, Davidson DF, Hanson RK. High-speed imaging of inhomogeneous ignition in a shock tube. Shock Waves 2018:1–7.